Drug Design, Development and Therapy

Dovepress
Taylor & Francis Group

Open Access Full Text Article

ORIGINAL RESEARCH

Paroxetine as a Therapeutic Agent in Inflammatory Osteolysis: Mechanistic Insights and Efficacy

Junming Huang[1–4,*], Zhipeng Wang[1–3,*], Jun Liu[1–3,*], Jihong Zhang[1–3], Kui Deng[1–3], Shanhu Huang[1–3], Song Zhou[1–3]

[1]The Orthopedic Hospital, The First Affiliated Hospital, Jiangxi Medical College, Nanchang University, Nanchang, Jiangxi, 330006, People's Republic of China; [2]Department of Sports Medicine, Orthopedic Hospital, The First Affiliated Hospital, Jiangxi Medical College, Nanchang University, Nanchang, Jiangxi, 330006, People's Republic of China; [3]The Key Laboratory of Spine and Spinal Cord Diseases of Jiangxi Province, Nanchang, Jiangxi, 330006, People's Republic of China; [4]Postdoctoral Research Station, The First Affiliated Hospital, Jiangxi Medical College, Nanchang University, Nanchang, Jiangxi, 330006, People's Republic of China

*These authors contributed equally to this work

Correspondence: Shanhu Huang; Song Zhou, Email hsh869@163.com; zhousong_tjmu@163.com

Background and Objective: Inflammatory osteolysis is a common feature of numerous orthopedic conditions, primarily driven by excessive osteoclast formation and activation. Recent studies have demonstrated that paroxetine, a selective serotonin reuptake inhibitor commonly prescribed for mental disorders, has significant anti-inflammatory effects. However, its effects on inflammatory osteolysis have not been fully elucidated. In this study, we investigated the effects and underlying mechanisms of paroxetine on osteoclast differentiation and function as well as its influence on inflammatory osteolysis in a murine model.

Methods: A mouse model of LPS-induced osteolysis was developed to assess the therapeutic efficacy of paroxetine in vivo. Utilizing the molecular structure of paroxetine, network pharmacology was used to predict principal targets and underlying mechanisms. The effect of paroxetine on osteoclast biology was subsequently investigated using morphological analysis, quantitative PCR (qPCR), and Western blotting.

Results: The findings from animal experiments demonstrated that paroxetine effectively mitigated LPS-induced bone loss by inhibiting osteoclast differentiation. In vitro analyses revealed that paroxetine suppresses osteoclast formation and bone resorption in a dose-dependent manner. Mechanistically, paroxetine downregulated osteoclast-specific genes and proteins while concurrently inhibiting the NF-κB and PI3K-AKT signaling pathways. Additionally, network pharmacology analysis identified PIK3CA as a pivotal target, substantiated by molecular docking studies (binding energy of −8.0 kcal/mol) and rescue experiments employing PI3K (740 Y-P) and AKT (SC79) agonists, which reversed paroxetine-mediated inhibition of osteoclast formation.

Conclusion: Paroxetine attenuated LPS-induced inflammatory osteolysis in mice and suppressed osteoclast differentiation and function in vitro, an effect associated with down-regulation of NF-κB and PI3K-AKT signaling. These data indicate that paroxetine may represent a potential therapeutic candidate for osteolytic bone diseases. However, further validation is required to confirm its efficacy and safety in more complex pre-clinical models and in humans.

Keywords: paroxetine, osteolysis, osteoclast, PIK3CA

Introduction

Throughout human lifespan, homeostasis of bone tissue is maintained through a finely tuned balance between bone resorption and bone formation. Osteoclasts are responsible for the removal of old or damaged bone followed by the synthesis of new bone tissue. Disruptions in the equilibrium of these processes can result in various bone diseases. Inflammatory osteolysis is primarily attributed to an increased number of osteoclasts and excessive bone resorption, which leads to reduced bone volume and bone formation disorders. This condition predominantly occurs in rheumatoid arthritis, psoriatic arthritis, orthopedic implant loosening, and osteomyelitis.[1] Therefore, the inhibition of osteoclastogenesis is a promising therapeutic approach for managing these conditions. However, existing pharmacological treatments

https://doi.org/10.2147/DDDT.S561725
Received: 22 September 2025
Accepted: 15 January 2026
Published: 27 January 2026

for osteoclast-mediated diseases, such as bisphosphonates and denosumab, are not only limited but are also linked to notable adverse effects. These side effects encompass gastrointestinal disturbances, atypical femoral fractures (AFF), osteonecrosis of the jaw (ONJ), atrial fibrillation, and severe infections.[2,3] In particular, prolonged use of bisphosphonates is associated with drug-induced ONJ and AFF.[4] Although denosumab is effective, it is expensive and carries the risk of rebound bone loss and multiple vertebral fractures upon discontinuation.[5] These challenges underscore the urgent need to develop alternative therapies that offer improved safety profiles and are more cost effective.

Osteoclasts are multinucleated giant cells differentiated from monocyte-macrophage lineage precursor cells that can adhere to the bone matrix and secrete acids and lytic enzymes to degrade mineralized matrices. Osteoclast differentiation is a complex process controlled by multiple cytokines and signaling pathways. Evidence from researchers has verified that osteoclast differentiation is mainly directed by two cytokines: Receptor Activator of Nuclear Factor κB ligand (RANKL) and Macrophage-Colony Stimulating Factor (M-CSF).[6] In the process of osteoclast differentiation, M-CSF promotes the proliferation and survival of bone marrow-derived macrophages (BMMs) and osteoclast precursors and stimulates RNAK expression, thereby increasing the activity of the RANK and RANKL complex.[7] RANKL is a crucial stimulator of osteoclast differentiation. It modulates essential processes, including precursor activation, fusion, and osteoclast survival through its interaction with the receptor RANK. This interaction recruits TNF receptor-associated factor 6 (TRAF6), which activates the downstream nuclear factor κB (NF-κB) signaling pathway. This cascade ultimately leads to the activation of nuclear factor of activated T-cells, cytoplasmic 1 (NFATc1), resulting in the upregulation of osteoclast-specific genes including tartrate-resistant acid phosphatase (TRAP), matrix metallopeptidase 9 (MMP-9), and cathepsin K (CTSK). Targeting the NF-κB pathway thus represents a viable strategy for inhibiting osteoclastogenesis, and identifying safe, clinically translatable agents that modulate this pathway is critical for advancing inflammatory osteolysis treatment.

Since its approval by the US Food and Drug Administration in 1992, paroxetine, a selective serotonin reuptake inhibitor, has been extensively employed in the management of a range of mental health disorders including depression, anxiety disorders, and post-traumatic stress disorder, and so on.[8] Recently, it has been reported that paroxetine can modulate diverse biological effects other than protection against psychiatric disorders. In patients with inflammatory bowel disease, paroxetine has shown the potential to alleviate intestinal inflammation by modulating the composition and functionality of the gut microbiota.[9] In addition, existing research indicates that paroxetine effectively inhibits the NF-κB pathway and mitigates the inflammatory response mediated by reactive microglia in astrocytes. In the context of the skeletal system, multiple studies focusing on arthritis have shown that paroxetine mitigates arthritis symptoms and reduces inflammatory responses, suggesting potential utility in bone-related inflammatory conditions.[10–12] Notably, paroxetine offers unique translational benefits due to its proven clinical safety, affordability, and oral bioavailability compared to new, untested drugs or existing osteolysis treatments. However, no studies have yet evaluated the role of paroxetine in inflammatory osteolysis, nor have they explored its translational potential as a repurposed agent for osteoclast-mediated bone destruction.

In this study, we aimed to evaluate the therapeutic efficacy of paroxetine on RANKL-stimulated osteoclastogenesis in vitro and inflammatory bone destruction in vivo, elucidate the underlying molecular mechanisms, and validate the translational potential of paroxetine as a repurposed agent for inflammatory osteolysis management.

Materials and Methods

Reagents

Recombinant mouse RANKL (462-TEC-010) and M-CSF (416-ML-010) were obtained from Bio-Techne (Minneapolis, MN). Paroxetine (HY-122272), SC79 (HY-18749), 740 Y-P (HY-P0175), and DMSO (dimethyl sulfoxide) (DMSO, HY-Y0320) were purchased from MedChemExpress (Monmouth Junction, NJ, USA). Alpha-MEM and fetal bovine serum (FBS) were obtained from HyClone (Marlborough, MA, USA), and the fluorescent dyes phalloidin (M21689) and DAPI (M5107) were obtained from AbMole (Houston, TX, USA).

Cells Isolation and Culture

As previously mentioned with minor modifications,[13,14] bone marrow cells were extracted from the femur and tibia and subsequently resuspended in red blood cell lysis buffer (Beyotime) for a duration of 2 minutes to facilitate the removal of red blood cells. The cells were then cultured in complete α-MEM supplemented with 30 ng/mL M-CSF in a suspension culture dish (Corning) at 37°C for three days. Following this incubation, non-adherent cells were eliminated by washing, and adherent bone marrow-derived macrophages (BMMs) were detached using 0.25% trypsin-EDTA (Thermo Fisher Scientific) for subsequent experimental procedures.

Cell Viability Assay

The BMMs were seeded overnight in 96-well plates at a density of 1×10^4cells/well density overnight. Subsequently, BMMs were treated with varying doses of paroxetine and DMSO for specified time periods. The cytotoxicity of paroxetine in BMMs was assessed using a CCK-8 kit (Target Molecule). Furthermore, BMMs cultured for 7 days were analyzed using the LIVE/DEAD Kit (Thermo Fisher Scientific) to measure cytotoxicity.

Osteoclast Differentiation and TRAP Staining

BMMs were cultured in induction media containing RANKL (100 ng/mL) with or without paroxetine. The medium was refreshed every alternate day until mature multinuclear osteoclasts appeared. TRAP staining was performed using a TRAP staining kit (Sigma-Aldrich) following the manufacturer's instructions. TRAP-positive cells with two or more nuclei were considered osteoclasts.

Immunofluorescent Staining of F-Actin Ring

BMMs were cultured in an induction medium with or without paroxetine until mature osteoclasts were formed. Cells were fixed for 30 min in 4% paraformaldehyde, permeabilized for 5 min using 0.1% Triton X-100, exposed to Phalloidin in PBS with 1% BSA for an hour to visualize F-actin, and stained with DAPI.

Bone Resorption Assay

BMMs were cultured in the presence of M-CSF and RANKL for five days to promote differentiation into mature osteoclasts. Following this period, the cultured cells were dissociated and transferred to a Bone Resorption Assay Plate, where they were further cultured in induction media with or without paroxetine for an additional four days. Subsequently, the cells were treated with a 10% sodium hypochlorite solution for 10 min to facilitate detachment from the plate. Images of the resorption pits were captured using a light microscope and quantified using ImageJ software.

Network Pharmacology Analysis

As previously mentioned with minor modifications,[15] the three-dimensional structural formula of paroxetine was retrieved from the PubChem database (https://pubchem.ncbi.nlm.nih.gov/) and used to identify and screen potential targets of paroxetine using the Swiss Target Prediction database (http://swisstargetprediction.ch). Multiple databases, including DrugBank (https://go.drugbank.com), GeneCards (https://www.genecards.org/), OMIM (https://omim.org/), the Therapeutic Target Database (TTD, http://db.idrblab.net/ttd/), and UniProtKB (https://www.uniprot.org/), were screened to identify targets related to osteolysis. Subsequently, both sets of targets were imported into Venny 2.1.0 platform to generate a Venn diagram. Common intersecting targets have been identified as potential targets for paroxetine in the treatment of osteolysis. To investigate the potential biological functions and key signaling pathways of paroxetine in the treatment of osteolysis, gene ontology (GO) and Kyoto Encyclopedia of Genes and Genomes (KEGG) enrichment analyses were independently performed on the prospective targets identified in Section 2.1.1, utilizing the DAVID databases (https://david.ncifcrf.gov/tools.jsp). Subsequently, the results of these analyses were visualized using an online bioinformatic platform (https://www.xiantaozi.com/).

Molecular Docking

As previously mentioned, with minor modifications,[16,17] the three-dimensional structure of paroxetine was acquired in SDF format from the PubChem database (https://pubchem.ncbi.nlm.nih.gov/), whereas the configuration of the target

protein was retrieved from the Protein Data Bank (PDB) (https://www.rcsb.org/) in PDB format. Molecular docking was performed using AutoDock version 4.2.3, and the resulting docking configuration with the lowest binding energy was saved in the pdbqt format. Docking results were visualized using PyMOL software. A docking binding energy of less than −6 kcal/mol indicates a strong binding affinity between the ligand and the protein.

RNA Isolation and Quantitative RT-PCR

BMMs were cultured in induction medium with or without paroxetine. In accordance with the manufacturer's instructions, total RNA was extracted from cells cultured for three days using the RNA-Quick Purification Kit (ESScience), followed by reverse transcription into complementary DNA (cDNA) using the Prime Script RT reagent kit (TaKaRa Biotechnology). The reverse-transcribed cDNA served as the template for quantitative real-time polymerase chain reaction (qRT-PCR), using SYBR (Vazyme) as the detection method. Appropriate internal control genes were used to normalize relative expression levels. The primer sequences used are listed in Table 1.

Western Blot Assay

To evaluate the role of paroxetine in the signaling pathways involved in osteoclast differentiation, BMMs were cultured in a culture dish for 24 h. Subsequently, BMMs were pretreated with DMSO or paroxetine for 2 h and stimulated with induction media for 0, 5, 15, and 45 min. To assess the effect of paroxetine on osteoclast differentiation, BMMs were cultured in induction medium supplemented with either vehicle (DMSO) or paroxetine for 3 days. Total protein samples were obtained by treating the cells with RIPA lysis buffer containing broad-spectrum phosphatase inhibitors and PMSF. Subsequently, protein concentration was determined using a BCA protein assay kit (Thermo Fisher Scientific). A quantity of 10μg of proteins was then subjected to electrophoresis on a 10% sodium dodecyl sulfate-polyacrylamide gel and subsequently transferred onto PVDF membranes (Millipore). After blocking with 5% non-fat milk, membranes were incubated with specific primary antibodies at 4 °C for an extended period. Subsequently, the membranes were washed with TBS-Tween and incubated with the corresponding horseradish peroxidase-conjugated secondary antibodies for 1 h at ambient temperature. Finally, the protein bands were identified using an electrochemical luminescence reagent (ECL) (Thermo Fisher Scientific) on a Bio-Rad system and analyzed using ImageJ software. Antibody information is listed in Supplementary Table 1.

Immunofluorescent Staining of p65

Immunofluorescence staining was performed to assess the effect of paroxetine on the nuclear translocation of p65. Specifically, cells were pre-incubated with paroxetine for 6 h and 30-minute treatment with RANKL. Subsequently, the cells were fixed, permeabilized, and blocked for 1 h with 1% bovine serum albumin (BSA). Thereafter, the cells were exposed to a primary antibody against p65 for 1 h, followed by incubation with an Alexa Fluor 488-conjugated secondary antibody for an additional hour. Finally, cell nuclei were visualized by staining with DAPI for 5 min. Images of p65 were obtained using a laser scanning confocal microscope.

Table 1 List of Primers Used in Quantitative Real-Time RT-PCR

Target Gene	Sense Sequence (5'to3')	Antisense Sequence (5'to3')
NFATc1	CAACGCCCTGACCACCGATAG	GGGAAGTCAGAAGTGGGTGGA
RANK	CAGGAGAGGCATTATGAGCA	GGTACTTTCCTGGTTCGCAT
TRAP	TACCTGTGTGGACATGACC	CAGATCCATAGTGAAACCGC
Cathepsin K	TGTATAACGCCACGGCAAA	GGTTCACATTATCACGGTCACA
c-Fos	CGGGTTTCAACGCCGACTA	TTGGCACTAGAGACGGACAGA
MMP9	CTGGACAGCCAGACACTAAAG	CTCGCGGCAAGTCTTCAGAG
GAPDH	AGGTCGGTGTGAACGGATTTG	TGTAGACCATGTAGTTGAGGTCA

Mouse Osteolysis Model and Pharmacological Interventions

All animal experiments were conducted under the supervision of the Animal Use and Care Committee of the First Affiliated Hospital of Nanchang University (CDYFY-IACUC-202311QR053) in accordance with the guidelines outlined in the NIH "Principles of Laboratory Animal Care" (1996 Revised Version). As previously mentioned, with minor modifications,[18,19] wild-type C57 BL /6 male mice, aged 8 weeks, were procured from SLAC Laboratory Animal Co. Ltd. (Shanghai, China) and housed in specific pathogen-free animal care facilities at the First Affiliated Hospital of Nanchang University. The mice were provided sterile chow and water and maintained under controlled environmental conditions, including a temperature of 25°C, humidity of 60%, and 12:12 light-dark cycle. Following the acclimatization period, the mice were randomly assigned to three groups (n=6): the control group (Control), mice that received lipopolysaccharide (LPS), and mice that received LPS treated with paroxetine (PA). Mice were intraperitoneally injected with LPS (5 mg/kg, Sigma-Aldrich, USA) on days 2 and 5 to induce osteolysis. Paroxetine was administered intraperitoneally at a dose of 20 mg/kg/day from day 1, in accordance with previous studies that demonstrated its non-toxicity in murine models.[11] Following a ten-day treatment period, all mice were euthanized with an overdose of pentobarbital and their femurs were harvested for further experimental analysis.

Bone Tissue Sample Analysis

The distal femur was scanned and analyzed using a micro-computed tomography (μ-CT) system (Scanco Medical) configured with a source voltage of 100 kV, source current of 98 mA, and resolution of 10.5 mm. The μ-CT and histomorphometric analysis protocols followed the methodology established in our previous study.[6,7,14,20,21] Specifically, the region of interest (ROI) for subsequent analysis was delineated as the area extending 0.5 mm below the subchondral bone. The femur underwent three-dimensional reconstruction, and the following parameters were assessed: bone volume-to-tissue volume ratio (BV/TV), trabecular number (Tb.N), trabecular thickness (Tb.Th), and trabecular separation (Tb.Sp). This analysis was performed using a software system integrated into the μ-CT device. Following μ-CT scanning, femurs were decalcified and embedded in paraffin. Coronal plane sections of the bone, measuring 5 μm in thickness, were prepared using a microtome and subjected to Hematoxylin and Eosin (H&E) or TRAP staining. In immunohistochemical staining, sections were deparaffinized, antigen retrieved, blocked and incubated with primary antibodies of p-p65 and p-AKT and corresponding biotinylated secondary antibodies. Then sections were stained with DAB and counterstained with haematoxylin. These procedures were conducted in accordance with our previously established methodologies.[7,21] Representative images of the trabecular region of the distal femur were captured and analyzed by microscopy.

Statistical Analysis

Each experiment was conducted with a minimum of three replicates, and the data are expressed as mean ± standard deviation (SD). For experiments involving more than two groups, statistical significance was assessed using one-way analysis of variance (ANOVA) followed by Tukey–Kramer honest significant difference (HSD) test. In experiments comparing two groups, unpaired t-tests were used to determine statistical significance. Statistical significance was set at $p < 0.05$.

Results

Paroxetine Attenuated LPS-Induced Bone Loss and Osteoclast Formation in vivo

To evaluate the therapeutic efficacy of paroxetine in the context of osteolysis, we administered LPS injection to simulate inflammatory osteolysis. Micro-CT analysis revealed a significant reduction in bone mass at the distal femur in the LPS group compared with that in the control group (Figure 1A). However, treatment with paroxetine effectively mitigated the bone loss associated with LPS stimulation. Detailed bone parameter analysis indicated a decrease in the bone volume-to-total volume ratio (BV/TV) and trabecular number (Tb.N), along with an increase in trabecular separation (Tb.Sp) in the LPS group. In contrast, the paroxetine-treated group exhibited a protective effect, characterized by increased BV/TV and Tb.N and decreased Tb.Sp (Figure 1B–E). These findings provide preliminary support to the hypothesis that paroxetine alleviates LPS-induced bone loss.

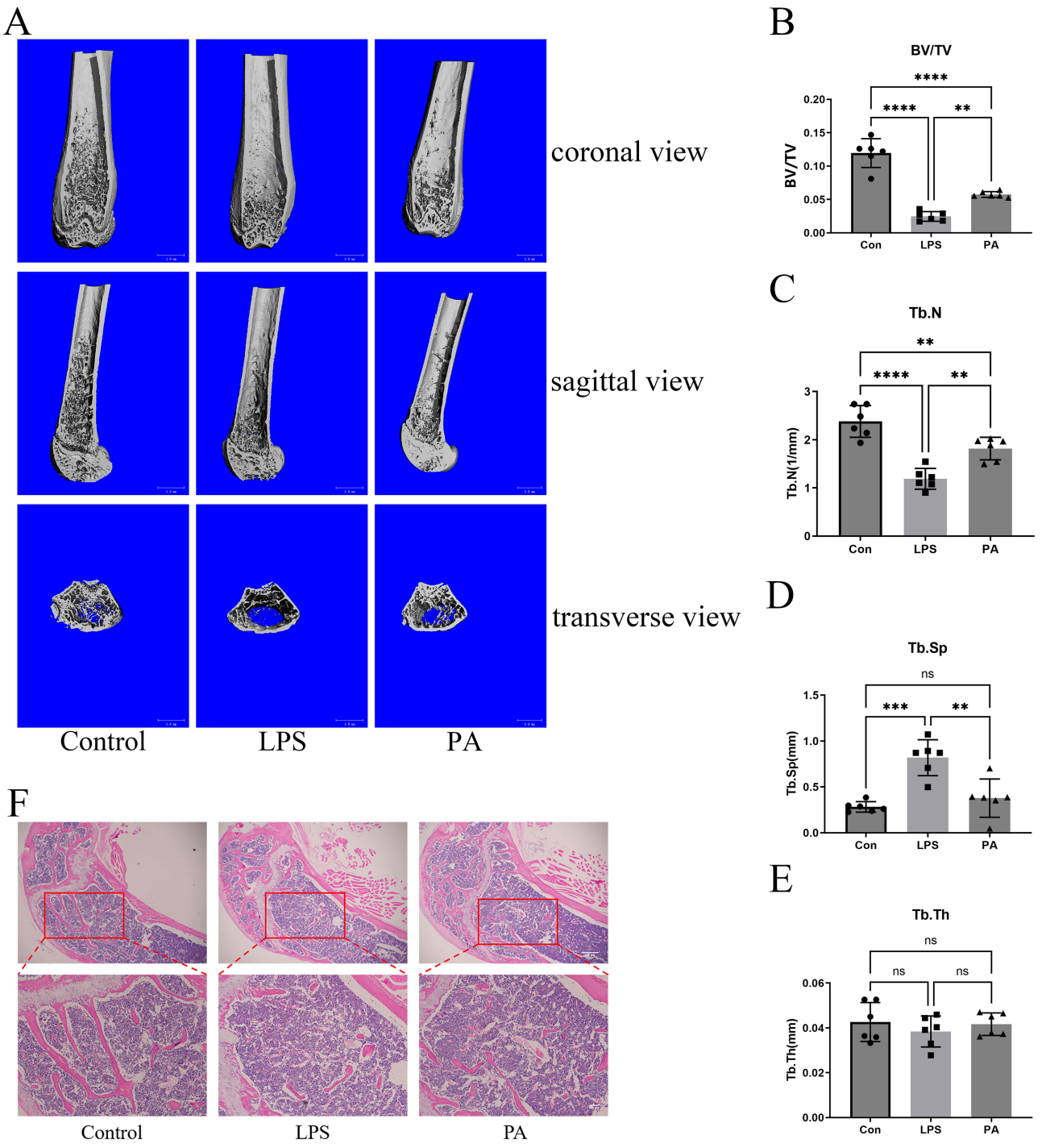

Figure 1 Paroxetine protests LPS-induced bone loss in vivo. (**A**) Reconstructed 3D micro-CT images representing the trabecular bone of the distal femoral metaphysis. (**B**) Morphometric parameters of trabecular structure: trabecular bone volume/tissue volume (BV/TV). (**C**) Morphometric parameters of trabecular structure: trabecular number (Tb.N). (**D**) Morphometric parameters of trabecular structure: trabecular separation (Tb.Sp). (**E**) Morphometric parameters of trabecular structure: trabecular thickness (Tb.Th). (**F**) Histopathology photographs of femoral samples after HE-stained sections. All bar graphs are presented as mean ± SD; n = 6. **P < 0.01; ***P < 0.001; ****P< 0.0001.
Abbreviation: ns, not statistical significance.

To further substantiate these findings, femurs obtained from the mice were dissected for histomorphometric analysis. As anticipated, H&E staining of the femoral tissue sections revealed that the trabeculae were sparse and thin in the distal femur region in the LPS group. In contrast, paroxetine treatment effectively mitigated bone loss, as evidenced by the presence of completely and orderly arranged trabeculae (Figure 1F). TRAP staining was performed to assess the effect of

https://doi.org/10.2147/DDDT.S561725

paroxetine on osteoclast formation in vivo. The increased number of osteoclasts per bone surface (N.Oc/BS) observed in the LPS group was significantly reduced following paroxetine administration (Figure 2).

Paroxetine Attenuates RANKL-Induced Osteoclast Differentiation in vitro

In our in vivo study, we demonstrated that the protective role of paroxetine could be attributed to its ability to suppress bone resorption. Consequently, we examined the effect of paroxetine on osteoclastogenesis by utilizing bone marrow-derived macrophages (BMMs) to induce osteoclast differentiation. Initially, we assessed the cytotoxicity of paroxetine on BMMs exposed to varying concentrations of paroxetine (0.625, 1.25, 2.5, 5, and 10 μM) for 24 or 72 h and observed no adverse effects on BMM proliferation up to a concentration of 2.5 μM (Figure 3A and B). Subsequently, we investigated the effect of paroxetine on RANKL-induced osteoclast formation. TRAP staining revealed that paroxetine inhibited osteoclastogenesis in a dose-dependent manner. Treatment with 1.25 or 2.5 μM paroxetine significantly reduced the number of TRAP-positive multinucleated cells (Figure 3C and D). To further explore the temporal effects of paroxetine on osteoclast formation, we continuously administered paroxetine (2.5 M) during the culture system during RANKL-induced osteoclast differentiation. Addition of paroxetine during the initial stages of differentiation (days 1–3) significantly inhibited osteoclast formation. In contrast, when bone marrow macrophages (BMMs) were exposed to paroxetine during days 3–5 or 5–7 of differentiation, there was also a reduction in the number of osteoclasts, although the inhibitory effect was less pronounced compared to that in the early stage (days 1–3) (Figure 3E and F). These findings suggested that paroxetine can inhibit osteoclast differentiation throughout the process, with the most substantial inhibitory effect observed when administered in the early stages.

Paroxetine Reduced Osteoclast-Mediated Bone Resorption in vitro

During osteoclast differentiation, F-actin rings are recognized as hallmark structures of mature osteoclasts and are essential for bone resorption activity. In alignment with the inhibition of osteoclast formation, the development of podosomal actin belts was disrupted, and a decrease in actin ring formation was observed in relation to the concentration of paroxetine administered (Figure 4A–C). Osteoclasts are the sole cell types responsible for bone resorption. Therefore, we evaluated the bone-resorptive function of osteoclasts following paroxetine treatment. The area of bone resorption significantly diminished in osteoclasts treated with paroxetine (Figure 4D and E).

Paroxetine Inhibited Expression Osteoclast-Specific Genes and Proteins

To further substantiate the inhibitory effect of paroxetine on osteoclast differentiation, we evaluated osteoclast-specific genes, including NFATc1, c-Fos, RANK, CTSK, MMP9, and TRAP, using qPCR. As anticipated, the relative mRNA

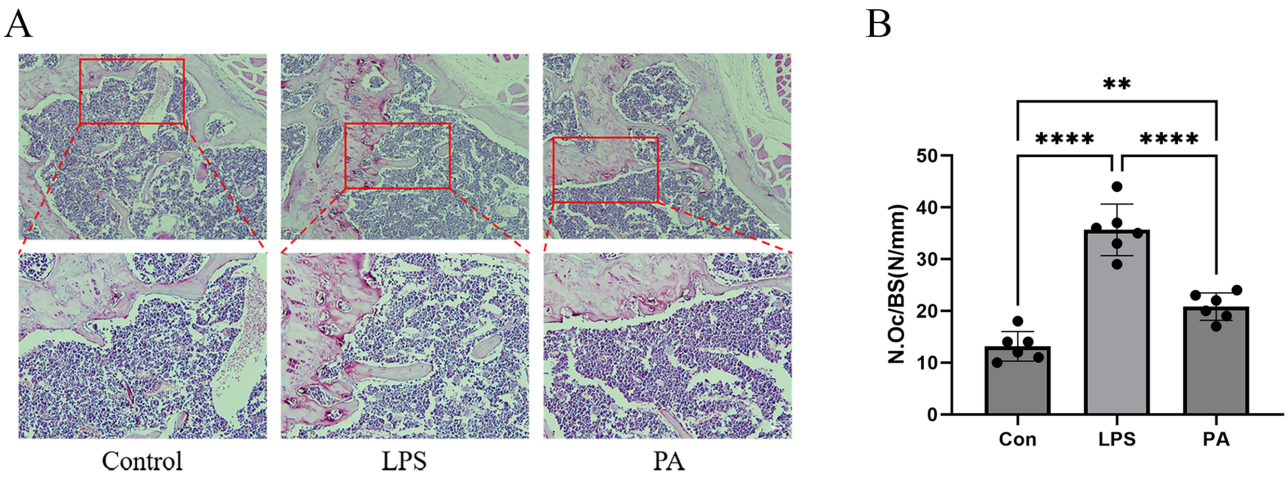

Figure 2 Paroxetine suppresses osteoclast differentiation in LPS-induced osteolytic model. (**A**) Histopathology photographs of femoral samples after TRAP-stained sections. (**B**) Quantitation of TRAP-positive cells on bone surface ratio (Oc.N/BS) in TRAP-stained sections. All bar graphs are presented as mean ± SD; n = 6. **P < 0.01; ****P< 0.0001.

https://doi.org/10.2147/DDDT.S561725

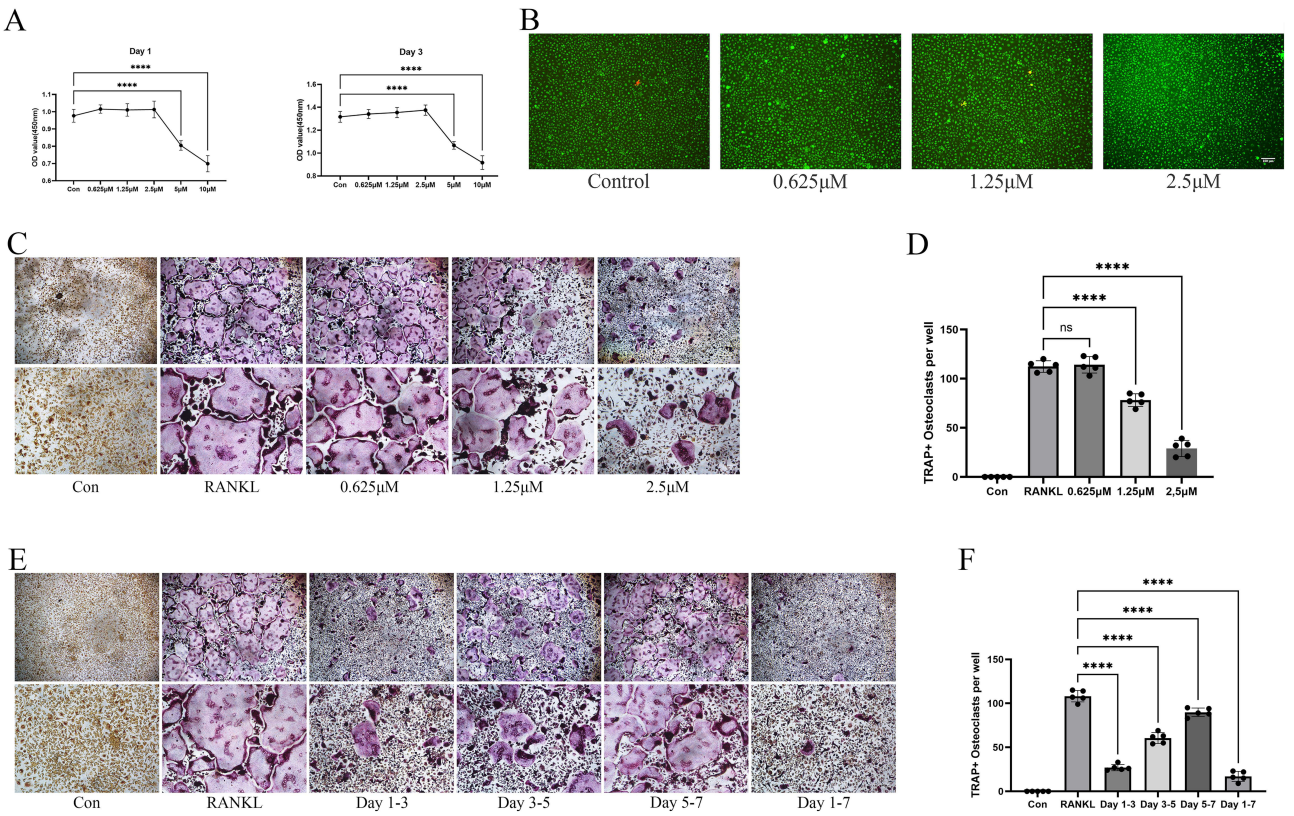

Figure 3 Paroxetine inhibits RANKL-mediated osteoclast differentiation in vitro. (**A**) CCK-8 assay was performed with different concentrations of paroxetine in BMMs for 1 day and 3 days. (**B**) The live/dead staining under different concentrations of paroxetine at day 3. (**C**) Representative TRAP staining images of RANKL-induced osteoclasts treated with different concentrations of paroxetine (upper: 200μm magnification, lower: 100μm magnification). (**D**) Quantitation of TRAP-positive cells after administration with different concentrations of paroxetine. (**E**) Representative TRAP staining images of RANKL-induced osteoclasts treated with paroxetine on specified days. (**F**) Quantitation of TRAP-positive cells after administration with paroxetine on specified days. All bar graphs are presented as mean ± SD; n = 5. ****P< 0.0001.
Abbreviation: ns, not statistical significance.

expression levels of these genes were upregulated following RANKL stimulation and subsequently suppressed by paroxetine in a concentration-dependent manner (Figure 5A). Western blot analysis corroborated the inhibitory trend observed in RT-PCR data. Specifically, the protein expression levels of NFATc1, c-fos, CTSK, and MMP9 were elevated following RANKL stimulation; however, paroxetine reduced this expression in a concentration-dependent manner (Figure 5B–E).

Paroxetine Inhibited RANKL-Induced Activation of the NF-κB Signaling Pathway

The NF-κB signaling pathway is involved in osteoclast differentiation. To ascertain whether paroxetine exerts regulatory effects on the RANKL-induced NF-κB pathway, Western blot experiments were conducted, which revealed that paroxetine significantly inhibited RANKL-induced phosphorylation of p65 and degradation of IκBα protein (Figure 6A and B). Additionally, immunofluorescence analysis was performed to elucidate the effects of paroxetine treatment on nuclear translocation of p65 in the NF-κB pathway. RANKL stimulation resulted in a substantial increase in the average nuclear fluorescence intensity of p65, an effect that was attenuated by paroxetine treatment (Figure 6C). Ultimately, the analysis of tissue samples demonstrated the expression of p-p65, indicating that paroxetine effectively downregulated P-p65 expression in bone tissue (Supplementary Figure 1). These findings are consistent with the results obtained from the cellular experiments.

Paroxetine Inhibited RANKL-Induced Phosphorylation of PI3K

To further elucidate the molecular mechanisms underlying the regulation of osteoclast differentiation by paroxetine, we employed network pharmacology to identify the potential therapeutic targets of paroxetine in the treatment of osteolysis.

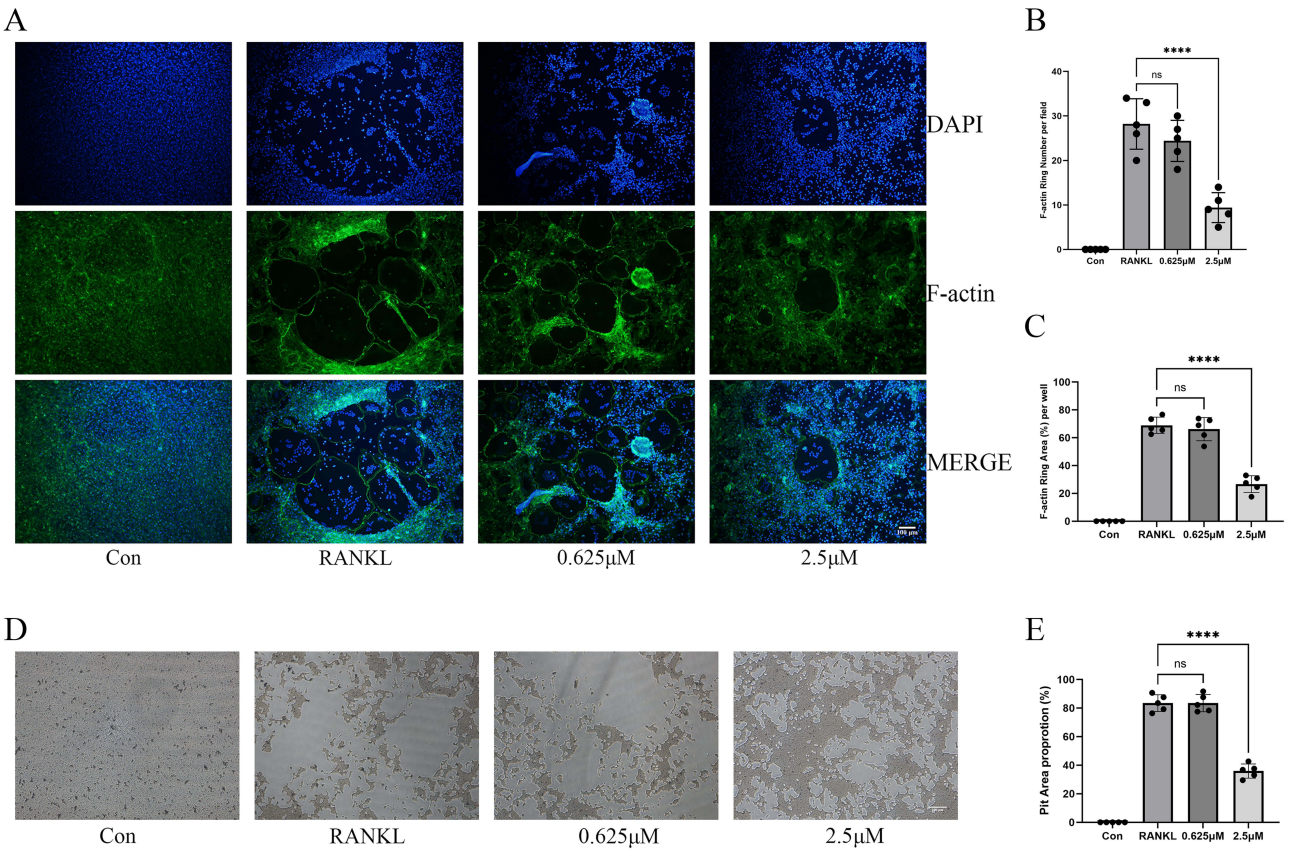

Figure 4 Paroxetine exhibits anti-resorption effect in vitro. (**A**) Representative images depicting podosome belts. (**B**) Quantification of the F-actin belt number of osteoclasts. (**C**) Quantification of the F-actin belt area of osteoclasts. (**D**) Representative images of bone resorptive areas of osteoclasts after administration with different concentrations of paroxetine. (**E**) Quantitation of bone resorptive areas. All bar graphs are presented as mean ± SD; n = 5. ****P< 0.0001.
Abbreviation: ns, not statistical significance.

Our analysis revealed 24 potential targets at the intersection of the paroxetine and osteolysis-related pathways. Notably, EGFR, PIK3CA, and PARP1 were the most relevant targets (Figure 7A and B). KEGG pathway enrichment analysis indicated a significant association between these targets and the PI3K-AKT signaling pathway. Concurrently, GO functional enrichment analysis highlighted their involvement in processes, such as phosphorylation modification and protein kinase activity (Figure 7C and D).

AKT plays an important role in osteoclast differentiation, and its activation is controlled by a multistep process involving phosphoinositide-3-kinase (PI3K), which comprises a regulatory subunit (p85α) and a catalytic subunit (p110α), with the catalytic subunit encoded by the PIK3CA gene. Thus, we aimed to investigate the regulatory effects of paroxetine on the PI3K-AKT signaling pathway during osteoclast differentiation. Western blot analyses demonstrated that paroxetine significantly inhibited RANKL-induced phosphorylation of PI3K as well as the subsequent phosphorylation of its downstream target AKT (Figure 8A and B). Simultaneously, we evaluated the expression of P-AKT in bone tissue, with findings similarly demonstrating that paroxetine inhibited P-AKT expression in this tissue (Supplementary Figure 2). Molecular docking studies revealed that paroxetine directly interacts with the binding domains of PI3KCA, exhibiting strong binding affinities with energies of −8.0 kcal/mol (Figure 8C and D). Furthermore, rescue experiments indicated that the application of PI3K (740 Y-P) and AKT (SC79) agonists effectively counteracted paroxetine-mediated inhibition of osteoclast differentiation (Figure 8E–H). These findings suggest that the PI3K-AKT signaling pathway plays a crucial role in the modulation of osteoclast differentiation by paroxetine.

https://doi.org/10.2147/DDDT.S561725

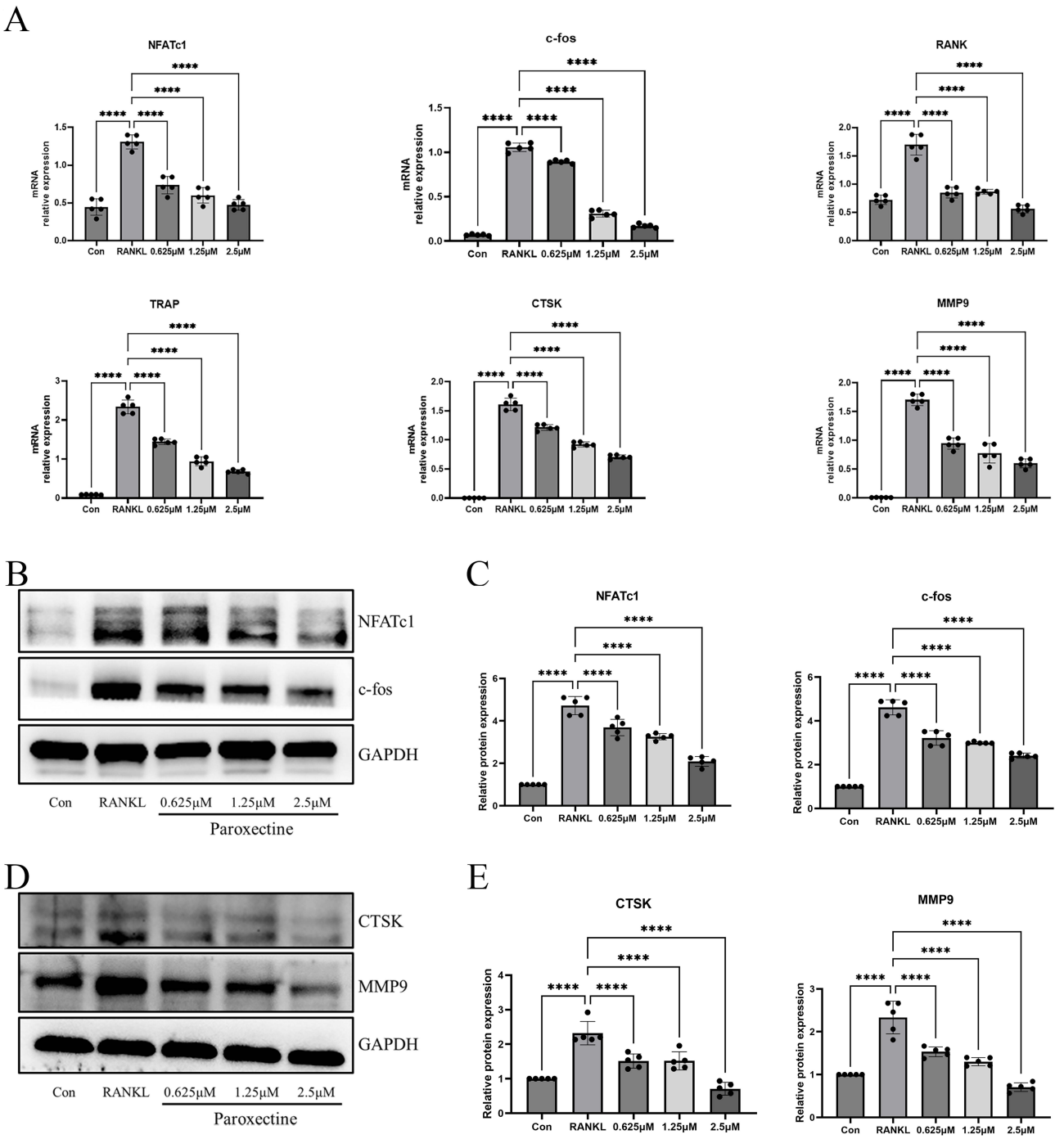

Figure 5 Paroxetine abrogates RANKL-induced NFATc1 and c-fos, and osteoclast-specific gene and protein expression in vitro. (**A**) Assessment of mRNA expression levels of osteoclastogenesis-associated marker genes after administration with paroxetine by RT-qPCR, including NFATc1, c-fos, RANK, TRAP, Cathepsin K, and MMP9. (**B**) Assessment of protein expression levels of NFATc1 and c-fos after administration with paroxetine by Western blot. (**C**) Quantitation of protein expression levels of NFATc1 and c-fos. (**D**) Assessment of protein expression levels of Cathepsin K and MMP9 after administration with paroxetine by Western blot. (**E**) Quantitation of protein expression levels of Cathepsin K and MMP9. All bar graphs are presented as mean ± SD; n = 5. ****P< 0.0001.

Discussion

Inflammatory bone resorption, characterized by the loss of bone mass due to inflammatory responses, is frequently associated with chronic inflammatory disorders such as Paget's disease, periodontitis, rheumatoid arthritis, metastatic cancer, and aseptic loosening of orthopedic implants.[22–24] These conditions can lead to various complications, including hypercalcemia, pain, and pathological fractures, thereby posing a significant global threat to public health and resulting in substantial social and

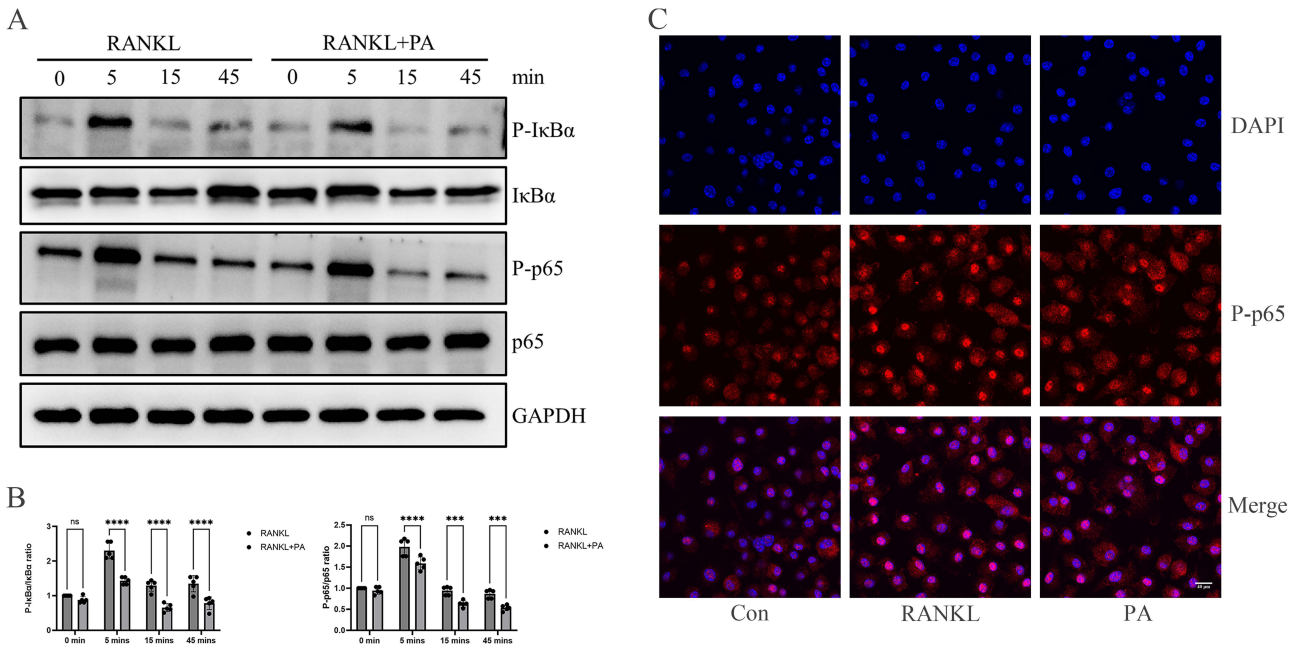

Figure 6 Paroxetine attenuates RANKL-mediated activation of NF-κB signaling pathway. (**A**) Assessment of phosphorylated level of IkB-α and p65 associated with RANKL stimulation by Western blot. (**B**) Quantitative analysis of phosphorylated IkB-α and p65 to total IkB-α and p65. (**C**) Representative fluorescence images of P65 nuclear translocation following RANKL stimulation without or with paroxetine. All bar graphs are presented as mean ± SD; n = 5. ***P < 0.001; ****P< 0.0001.
Abbreviation: ns, not statistical significance.

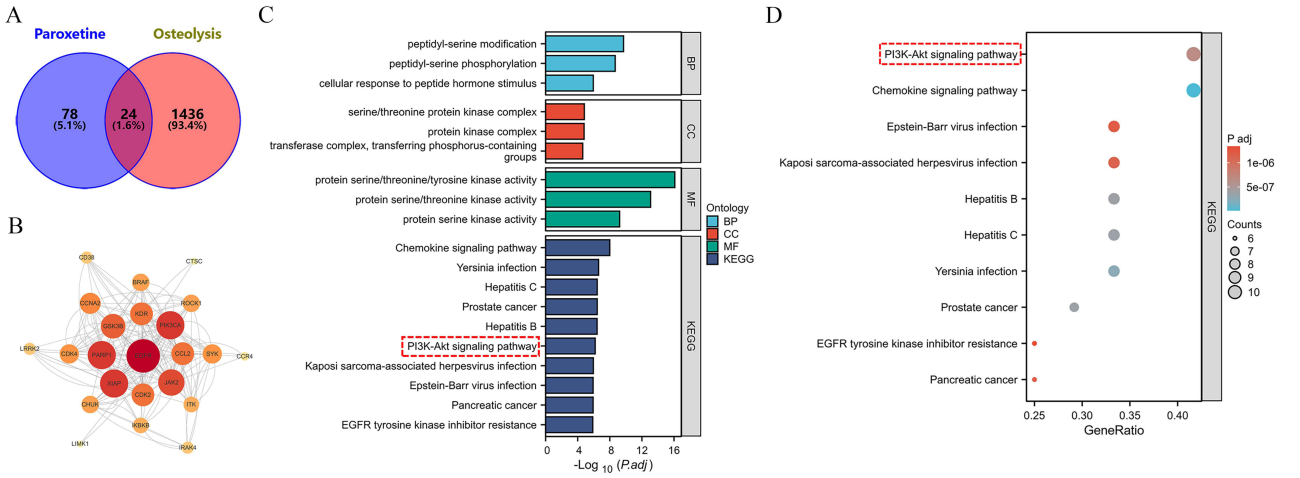

Figure 7 Network pharmacology analysis of paroxetine against osteolysis. (**A**) Venn diagram of osteolysis-associated genes and paroxetine-binding candidates, yielding 24 intersecting targets used for downstream analyses. (**B**) PPI network of the 24 intersecting targets, with node size proportional to degree centrality and the top 10 hub genes outlined by red dotted borders. (**C**) Histogram of GO (BP biological process, CC cellular component, MF molecular function) and KEEG enrichment results for intersecting targets between paroxetine and osteolysis based on the P value. (**D**) Bubble diagram of top 10 KEEG pathways for intersecting targets between paroxetine and osteolysis sorted by gene counts.

economic impacts. Osteoclast activity is crucial for maintaining bone homeostasis. However, excessive activation has been linked to numerous osteolytic diseases. Therefore, targeting the inhibition of osteoclast activity and differentiation represents a promising strategy for alleviating inflammatory bone destruction associated with these disorders.

Current pharmacological management of osteolytic disorders is dominated by drugs that inhibit osteoclast-mediated bone resorption. Despite their efficacy, these medications are associated with considerable adverse effects, and the discovery and development of novel therapeutics is protracted and uncertain. Consequently, there is growing interest in old drugs, which were originally developed for non-skeletal indications but have recently been discovered to modulate

https://doi.org/10.2147/DDDT.S561725

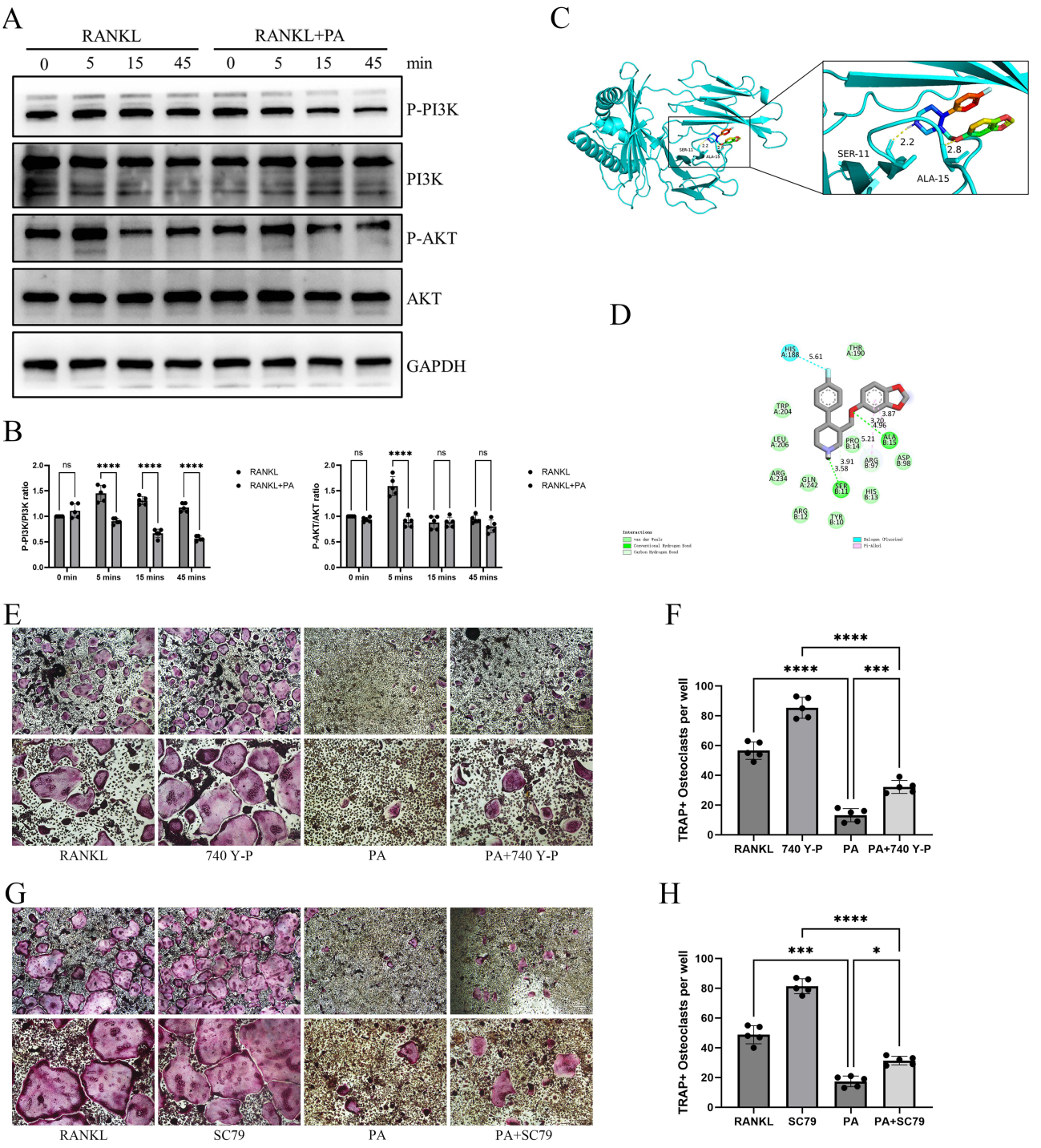

Figure 8 Paroxetine antagonize RANKL-mediated activation of PI3K-AKT signaling pathway through targeting PIK3CA. (**A**) Assessment of phosphorylated level of PI3K and AKT associated with RANKL stimulation by Western blot. (**B**) Quantitative analysis of phosphorylated PI3K and AKT to total PI3K and AKT. (**C**) The 3D images of molecular docking between paroxetine and PIK3CA. (**D**) The 2D docking diagrams specifically highlight the hydrogen bonding sites of paroxetine and PIK3CA. (**E**) Representative TRAP staining images of RANKL-induced osteoclasts administrated with paroxetine and PI3K agonist (740 Y-P). (**F**) Quantitation of TRAP-positive cells after administration with paroxetine and PI3K agonist (740 Y-P). (**G**) Representative TRAP staining images of RANKL-induced osteoclasts administrated with paroxetine and AKT agonist (SC79). (**H**) Quantitation of TRAP-positive cells after administration with paroxetine and AKT agonist (SC79). All bar graphs are presented as mean ± SD; n = 5. *P < 0.05; ***P < 0.001; ****P< 0.0001.

Abbreviation: ns, not statistical significance.

https://doi.org/10.2147/DDDT.S561725

bone turnover. The emerging concept of "old drugs with new tricks" in bone metabolism is exemplified by several well-characterized compounds, such as tamsulosin, propranolol, and tetracycline antibiotics.[25–27]

In this study, we provide the first comprehensive evidence that paroxetine, a selective serotonin reuptake inhibitor safely prescribed for depression and anxiety for more than three decades, exhibits significant anti-osteoclastogenic and anti-resorptive effects both in vitro and in vivo, and effectively reduces bone loss in an inflammatory osteolysis model. Mechanistically, paroxetine concurrently disrupted the RANKL-induced NF-κB signaling pathway and PI3K-AKT axis, both of which are crucial for osteoclast differentiation and function. These findings not only broaden the pharmacological applications of paroxetine beyond its traditional psychiatric use but also suggest it as a promising candidate for repurposing in the treatment of osteolytic diseases.

Osteoclast differentiation is a complex process involving numerous cytokines, and the RANKL-RANK axis plays a critical role under normal physiological conditions.[28] Upon stimulation by RANKL, the cytoplasmic domain of RANK recruits TRAF6, initiating multiple signaling pathways that enhance c-Fos levels and modulate the interaction between c-Fos and NFATc1, a master transcription factor that regulates osteoclast activity. RANKL induces the NF-κB pathway, induced by RANKL, is pivotal for osteoclast development and pathological osteolysis.[7] The NF-κB kinase complex is assembled in response to RANKL stimulation, leading to the phosphorylation and degradation of the NF-κB repressor protein IκBα. This process facilitates the translocation of p65 from the cytoplasm to the nucleus, thereby initiating transcription of osteoclast-specific genes. Our data indicate that paroxetine suppressed the phosphorylation of IκBα and p65, reducing the nuclear accumulation of p65. These findings suggest that paroxetine inhibits the phosphorylation of the NF-κB signaling pathway, thereby impeding osteoclast formation and function.

Next, we performed network pharmacology analysis to identify PIK3CA as a potential therapeutic target for paroxetine in the treatment of osteolysis. Bioinformatics enrichment analysis also implicates the PI3K-AKT axis as an additional node through which paroxetine restrains osteoclastogenesis. PIK3CA encodes the catalytic subunit p110α of class I phosphoinositide 3-kinase (PI3K), a pivotal lipid kinase in the PI3K-AKT signaling pathway. Upon activation by ligand binding to receptor tyrosine kinases or G-protein-coupled receptors, p110α is translocated to the plasma membrane, where it catalyzes the conversion of phosphatidylinositol-4,5-bisphosphate (PIP2) into phosphatidylinositol-3,4,5-trisphosphate (PIP3). PIP3 serves as a crucial secondary messenger that facilitates the recruitment and subsequent phosphorylation of AKT. Once fully activated, AKT phosphorylates a wide array of downstream protein substrates, thereby promoting cellular differentiation.[29] In the regulation of bone metabolism, the activation of PI3K/AKT signaling facilitates the proliferation and survival of BMMs and augments their responsiveness to RANKL, thereby enhancing their capacity to differentiate into mature osteoclasts. Furthermore, AKT activation induces the phosphorylation and activation of transcription factors implicated in osteoclast differentiation, including c-Fos, NFATc1, and NF-κB, which in turn enhance the expression of osteoclast-specific genes and further promote osteoclastogenesis.[30–32] In this study, we demonstrated that paroxetine inhibits the phosphorylation of PI3K and AKT, thereby attenuating the activity of the PI3K-AKT signaling pathway. Moreover, the application of the PI3K agonist 740 Y-P or the AKT activator SC79 reversed the paroxetine-induced inhibition of osteoclast formation. These findings suggest that the inhibitory effect of paroxetine on osteoclast formation is dependent on the PI3K-AKT pathway.

Lipopolysaccharide (LPS), a bacterial endotoxin, has been extensively utilized in studies of inflammatory bone resorption owing to its capacity to stimulate the production of inflammatory mediators, leading to osteoclast overactivation and subsequent bone resorption. In this study, we used an in vivo mouse model to investigate the effects of paroxetine on LPS-induced femoral bone destruction. Our findings demonstrated that paroxetine effectively mitigated bone destruction, aligning with its pronounced inhibitory effect on osteoclast formation and function observed in vitro. H&E staining revealed substantial bone loss in the LPS-treated cohort, whereas TRAP staining indicated increased osteoclast population in the femoral region. Notably, paroxetine administration significantly reduced the number of TRAP-positive cells and effectively attenuated the LPS-induced bone resorption. The protective mechanism of paroxetine against LPS-induced bone resorption is likely due to its ability to inhibit osteoclast differentiation and function.

Despite these promising results, several questions remain unanswered. First, functional equilibrium between osteoblasts and osteoclasts is crucial for maintaining normal bone mass. The present study focused exclusively on inhibitory effects of paroxetine on osteoclast differentiation and function, but did not assess its potential impacts on osteoblast

biology. This constitutes a critical limitation, as the therapeutic utility of a bone-targeting agent cannot be fully evaluated without accounting for its effects on both cell lineages. The chronic use of selective serotonin reuptake inhibitors has been linked to modest reductions in bone mineral density in epidemiological studies, a phenomenon attributed to serotonin receptors and transporters.[33–35] It remains to be determined whether this effect counterbalances the anti-osteolytic effects of paroxetine observed in this study, necessitating further investigation using long-term, large animal models. Furthermore, although the LPS-induced osteolysis model offers advantages of rapid induction and high reproducibility, it predominantly mimics acute systemic inflammation rather than the chronic autoimmune milieu typical of rheumatoid arthritis or the foreign-body reactions linked to orthopedic implant loosening. To comprehensively verify therapeutic efficacy of paroxetine across diverse inflammatory etiologies of osteolysis, future studies should integrate K/BxN serum transfer, collagen-induced arthritis (CIA), and titanium particle-induced osteolysis models. Finally, although PIK3CA has been recognized as a potential target for the modulation of osteoclast differentiation by paroxetine, the precise molecular mechanisms governing this regulation require further investigation.

In conclusion, paroxetine exhibits potential in alleviating inflammatory osteolysis by concurrently inhibiting the NF-κB and PI3K-AKT signaling pathways, thereby suppressing osteoclast differentiation and activity. However, this conclusion is constrained by the use of an acute LPS model (which does not recapitulate chronic clinical contexts), the unassessed effects on osteoblast function (a key component of bone homeostasis), and the need for deeper mechanistic exploration of PIK3CA-mediated regulation. Thus, paroxetine may serve as a candidate for further investigation into osteolytic bone disease treatment, with its clinical applicability requiring validation in more relevant models and comprehensive assessments of bone metabolism balance.

Data Sharing Statement

The datasets generated and/or analyzed during the current study are available upon reasonable request to the corresponding author Song Zhou (zhousong_tjmu@163.com).

Ethics Approval

All the animal experiments were conducted under the supervision of the Animal Use and Care Committee of the First Affiliated Hospital of Nanchang University (CDYFY-IACUC-202311QR053).

Author Contributions

All authors made a significant contribution to the work reported, whether that is in the conception, study design, execution, acquisition of data, analysis and interpretation, or in all these areas; took part in drafting, revising or critically reviewing the article; gave final approval of the version to be published; have agreed on the journal to which the article has been submitted; and agree to be accountable for all aspects of the work.

Funding

This work was supported by research grants from the National Natural Science Foundation of China (82300994 82560183 81560352), Key Research and Development Program of Jiangxi Province (20223BBG71S02), Natural Science Foundation of Jiangxi Province (20232BAB216034 20171BAB205031 20181ACB20024), and the China Postdoctoral Science Foundation (2023M741520).

Disclosure

The authors declare no competing interests associated with this study.

References

1. Yu Z-C, Fu R, Li Y, Zhao D-Y, Jiang H, Han D. The STING inhibitor C-176 attenuates osteoclast-related osteolytic diseases by inhibiting osteoclast differentiation. *THE FASEB Journal*. 2023;37(4):e22867. doi:10.1096/fj.202201600R
2. Querrer R, Ferrare N, Melo N, et al. Differences between bisphosphonate-related and denosumab-related osteonecrosis of the jaws: a systematic review. *Support Care Cancer*. 2021;29(6):2811–2820. doi:10.1007/s00520-020-05855-6

3. Clézardin P, Coleman R, Puppo M, et al. Bone metastasis: mechanisms, therapies, and biomarkers. *Physiol Rev*. 2021;101(3):797–855. doi:10.1152/physrev.00012.2019
4. Matuoka JY, Kahn JG, Secoli SR. Denosumab versus bisphosphonates for the treatment of bone metastases from solid tumors: a systematic review. *Eur J Health Econ*. 2019;20(4):487–499. doi:10.1007/s10198-018-1011-1
5. Kendler DL, Cosman F, Stad RK, Ferrari S. Denosumab in the treatment of osteoporosis: 10 years later: a narrative review. *Adv Ther*. 2022;39(1):58–74. doi:10.1007/s12325-021-01936-y
6. Ma M, Fan AY, Liu Z, et al. Baohuoside I inhibits osteoclastogenesis and protects against ovariectomy-induced bone loss. *Front Pharmacol*. 2022;13:874952. doi:10.3389/fphar.2022.874952
7. Huang JM, Wang CZ, Lu SY, Wang Z, Yan ZQ. Oroxin B attenuates ovariectomy-induced bone loss by suppressing osteoclast formation and activity. *Drug Des Devel Ther*. 2021;15:4811–4825. doi:10.2147/dddt.S328238
8. Kowalska M, Nowaczyk J, Ł F, Nowaczyk A. Paroxetine-overview of the molecular mechanisms of action. *Int J Mol Sci*.;224:10.3390/ijms22041662
9. Ning L, Wang X, Xuan B, et al. Identification and investigation of depression-related molecular subtypes in inflammatory bowel disease and the anti-inflammatory mechanisms of paroxetine. *Front Immunol*. 2023;14:1145070. doi:10.3389/fimmu.2023.1145070
10. Tai Y, Huang B, Guo PP, et al. TNF-α impairs EP4 signaling through the association of TRAF2-GRK2 in primary fibroblast-like synoviocytes. *Acta Pharmacol Sin*. 2022;43(2):401–416. doi:10.1038/s41401-021-00654-z
11. Zheng X, Qiu J, Gao N, et al. Paroxetine attenuates chondrocyte pyroptosis and inhibits osteoclast formation by inhibiting nf-κb pathway activation to delay osteoarthritis progression. *Drug Des Devel Ther*. 2023;17:2383–2399. doi:10.2147/dddt.S417598
12. Carlson EL, Karuppagounder V, Pinamont WJ, et al. Paroxetine-mediated GRK2 inhibition is a disease-modifying treatment for osteoarthritis. *Sci Transl Med*. 13(580) doi:10.1126/scitranslmed.aau8491
13. Chen K, Ng PY, Chen R, et al. Sfrp4 repression of the Ror2/Jnk cascade in osteoclasts protects cortical bone from excessive endosteal resorption. *Proc Natl Acad Sci U S A*. 2019;116(28):14138–14143. doi:10.1073/pnas.1900881116
14. Chen K, Chen X, Lang C, et al. CircFam190a: a critical positive regulator of osteoclast differentiation via enhancement of the AKT1/HSP90β complex. *Exp Mol Med*. 2023;55(9):2051–2066. doi:10.1038/s12276-023-01085-y
15. Lu Q, Wang H, Zhang X, et al. Corydaline attenuates osteolysis in rheumatoid arthritis via mitigating reactive oxygen species production and suppressing calcineurin-Nfatc1 signaling. *Int Immunopharmacol*. 2024;142(Pt B):113158. doi:10.1016/j.intimp.2024.113158
16. Tan L, Miao Z, Zhao Y, et al. Dual regulation of phaseol on osteoclast formation and osteoblast differentiation by targeting TAK1 kinase for osteoporosis treatment. *J Adv Res*. 2024. doi:10.1016/j.jare.2024.12.009
17. Wang Z, Deng W, Tang K, et al. Isoginkgetin Inhibits RANKL-induced osteoclastogenesis and alleviates bone loss. *Biochem Pharmacol*. 2025;231:116673. doi:10.1016/j.bcp.2024.116673
18. Zhang L, Yu Z, Zhu Y, et al. Pegylation enhances the anti-osteoporosis activity of acacetin in both ovariectomized and LPS-stimulated mice. *Bioorg Med Chem*. 113. 117910. doi:10.1016/j.bmc.2024.117910
19. Jin Y, Wang Y, Wang C, et al. Salidroside inhibits osteoclast differentiation based on osteoblast-osteoclast interaction via HIF-1a pathway. *Chin J Nat Med*. 2025;23(5):572–584. doi:10.1016/s1875-5364(25)60864-8
20. Huang JM, Ren RY, Bao Y, et al. Ulinastatin inhibits osteoclastogenesis and suppresses ovariectomy-induced bone loss by downregulating uPAR. *Front Pharmacol*. 2018;9:1016. doi:10.3389/fphar.2018.01016
21. Huang J, Ma T, Wang C, et al. SOST/Sclerostin impairs the osteogenesis and angiogesis in glucocorticoid-associated osteonecrosis of femoral head. *Mol Med*. 30(1):167. doi:10.1186/s10020-024-00933-5
22. Osteoimmunology GR. Inflammatory osteolysis and regeneration of the alveolar bone. *J Clin Periodontol*. 2019;46(21):52–69. doi:10.1111/jcpe.13056
23. Eger M, Hiram-Bab S, Liron T, et al. Mechanism and Prevention of Titanium Particle-Induced Inflammation and Osteolysis. *Front Immunol*. 2018;9:2963. doi:10.3389/fimmu.2018.02963
24. Law YY, Rengamanar H, Wu CY, et al. Ugonin P mitigates osteolytic bone metastasis by suppressing MDK via upregulating miR-223-3p expression. *Int J Biol Sci*. 2025;21(8):3740–3754. doi:10.7150/ijbs.111356
25. Li S, Sun W, Li S, et al. Tamsulosin ameliorates bone loss by inhibiting the release of Cl(-) through wedging into an allosteric site of TMEM16A. *Proc Natl Acad Sci U S A*. 2025;122(1):e2407493121. doi:10.1073/pnas.2407493121.
26. Treyball A, Bergeron AC, Brooks DJ, et al. Propranolol promotes bone formation and limits resorption through novel mechanisms during anabolic parathyroid hormone treatment in female C57BL/6J mice. *J Bone Miner Res*. 2022;37(5):954–971. doi:10.1002/jbmr.4523
27. Warner AJ, Hathaway-Schrader JD, Lubker R, Davies C, Novince CM. Tetracyclines and bone: unclear actions with potentially lasting effects. *Bone*. 2022;159:116377. doi:10.1016/j.bone.2022.116377
28. De Leon-Oliva D, Barrena-Blázquez S, Jiménez-álvarez L, et al. The RANK-RANKL-OPG System: a Multifaceted Regulator of Homeostasis, Immunity, and Cancer. *Medicina*. 2023;59(10). doi:10.3390/medicina59101752
29. Yu L, Wei J, Liu P. Attacking the PI3K/Akt/mTOR signaling pathway for targeted therapeutic treatment in human cancer. *Semin Cancer Biol*. 2022;85:69–94. doi:10.1016/j.semcancer.2021.06.019
30. Li J, Wei JJ, Wu CH, et al. Epimedin A inhibits the PI3K/AKT/NF-κB signalling axis and osteoclast differentiation by negatively regulating TRAF6 expression. *Mol Med*. 2024;30(1):125. doi:10.1186/s10020-024-00893-w
31. Meng J, Zhang W, Wang C, et al. Catalpol suppresses osteoclastogenesis and attenuates osteoclast-derived bone resorption by modulating PTEN activity. *Biochem Pharmacol*. 2020;171:113715. doi:10.1016/j.bcp.2019.113715
32. Wu Z, Li X, Chen X, et al. Phosphatidyl Inositol 3-Kinase (PI3K)-Inhibitor CDZ173 protects against LPS-induced osteolysis. *Front Pharmacol*. 2022;13:1021714. doi:10.3389/fphar.2022.1021714
33. Feuer AJ, Demmer RT, Thai A, Vogiatzi MG. Use of selective serotonin reuptake inhibitors and bone mass in adolescents: an NHANES study. *Bone*. 2015;78:28–33. doi:10.1016/j.bone.2015.04.042
34. Zhou C, Fang L, Chen Y, Zhong J, Wang H, Xie P. Effect of selective serotonin reuptake inhibitors on bone mineral density: a systematic review and meta-analysis. *Osteoporos Int*. 2018;29(6):1243–1251. doi:10.1007/s00198-018-4413-0
35. Kang S, Han M, Park CI, et al. Use of serotonin reuptake inhibitors and risk of subsequent bone loss in a nationwide population-based cohort study. *Sci Rep*. 2021;11(1):13461. doi:10.1038/s41598-021-92821-9.